Physical Science International Journal

23(1): 1-20, 2019; Article no.PSIJ.50248
ISSN: 2348-0130

Dilation of Time and Newton's Absolute Time

Stefan Von Weber[1*] and Alexander Von Eye[2]

[1]Hochschule Furtwangen University, Germany.
[2]Michigan State University, USA.

Authors' contributions

This work was carried out in collaboration between the both authors. Author SVW designed the study and programmed the computations. Author AVE gave mathematical and physical support. Both authors contributed equally to this work and read and approved the final manuscript.

Article Information

DOI: 10.9734/PSIJ/2019/v23i130141
Editor(s):
(1) Dr. Lei Zhang, Winston-Salem State University, North Carolina, USA.
(2) Dr. Christian Brosseau, Distinguished Professor, Department of Physics, Université de Bretagne Occidentale, France.
Reviewers:
(1) Francisco Bulnes, TESCHA, Mexico.
(2) Snehadri Ota, Institute of Physics, India.
(3) A. Ayeshamariam, Khadir Mohideen College, India.
(4) Christian Parigger, University of Tennessee, USA.
(5) Orchidea Maria Lecian, Sapienza University, Italy.
Complete Peer review History: http://www.sdiarticle3.com/review-history/50248

Original Research Article

Received 14 May 2019
Accepted 30 July 2019
Published 13 August 2019

ABSTRACT

The Cosmic Membrane theory states that the space in which the cosmic microwave background radiation has no dipole is identical with Newton's absolute space. Light propagates in this space only. In contrast, in a moving inertial frame of reference light propagation is in-homogeneous, i.e. it depends on the direction. Therefore, the derivation of the dilation of time in the sense of Einstein's special relativity theory, i.e., together with the derivation of the length contraction under the constraint of constant cross dimensions, loses its plausibility, and one has to search for new physical foundations of the relativistic contraction and dilation of time. The Cosmic Membrane theory states also that light paths remain always constant independent on the orientation and the speed of the moving inertial frame of reference. Effects arise by the dilation of time. We predict a long term effect of the Kennedy-Thorndike experiment, but we show also that this effect is undetectable with today's means. The reason is that the line width of the light sources hides the effect. The use of lasers, cavities and Fabry-Pérot etalons do not change this. We propose a light clock of special construction that could indicate Newton's absolute time t_0 nearly precisely.

**Corresponding author: E-mail: webers@hs-furtwangen.de, Stefan.vonWeber@hs-furtwangen.de;*

Keywords: Dilation of time; relativity; membrane; absolute space; Kennedy-Thorndike experiment.

1. INTRODUCTION

In the Cosmic Membrane theory (CM), time is connected with the 4-th dimension of space, *w* ($w=V_E\ t$). The quantity V_E is the speed of expansion of the cosmic membrane, similar to the construction $-ct$ of Einstein's relativity. The dilation of time of moving clocks holds in the CM for each movement in the absolute space. In the case of earth-bound clocks, we need to consider, besides the speed of the galaxy, the speed of the Sun, the movement of the Earth around the Sun and the rotation of the Earth in addition to the influence of the gravitational field in form of the gravitational red-shift. Because of the fact that the Earth as moving body is subject both to the relativistic change of mass and to the relativistic contraction, earth-bound clocks are imposed to influences of manifold nature, which are difficult to separate that.

In the CM, dilation of time formally equals the dilation of time in Einstein's special relativity theory (SR), i. e.

$$t' = t_0 / \sqrt{1-\beta^2}\ . \tag{1.1}$$

Here, $\beta=v/c$, with v being the speed of the clock in the absolute space, and c being the speed of light. The time t_0 is Newton's absolute time, indicated by a clock that rests in absolute space and is not under the influence of a gravitational field. The relation of Eq. (1.1) has been proven sufficiently accurately in several experiments, first by Stilwell in 1938 [1]. Another Ives-Stilwell-type time dilation experiment [2] using 7Li+ ions confirmed at a velocity of β=v/c=0.338 in the storage ring ESR at Darmstadt the time dilation factor γ to within $\pm 2.3\times10^{-9}$. Häfele and Keating [3] gave an indirect prove. The contraction of length of moving bodies is, in the SR,

$$l' = l\sqrt{1-\beta^2}\ . \tag{1.2}$$

This relation has been never verified experimentally. However, both relations (Eq. 1.1 and Eq. 1.2) play an important role in the Lorentz-transform, and therefore also in the SR. A common derivation of the two equations, Eq. 1.1 and Eq. 1.2, is based on the postulate of the SR that the light of a light source is spreading with speed c in each direction in each inertial frame of reference, i. e. it has always the form of a spherical wave. It holds:

$$x^2+y^2+z^2-(ct)^2 = x'^2+y'^2+z'^2-(ct')^2\ . \tag{1.3}$$

Here, x, y, and z are the coordinates, t is the time in the first inertial frame of reference, and x', y', and z' are the coordinates, and t' the time in the second inertial frame of reference. The second frame of reference has the constant speed v relative to the first inertial frame of reference. The x-axis and the x'-axis, respectively, point in the same direction without restriction of generality. With the another postulate – the cross-dimensions that are perpendicular to the speed vector v of the moving body in the two inertial frames of reference remain unchanged – one ultimately obtains the above two equations (Eq. 1.1 and Eq. 1.2). Therefore, the dilation of time and the length contraction are inseparably linked by this derivation.

However, since the discovery of the Cosmic Microwave Background Radiation (CMBR) by Wilson and Penzias [4] we know that there exists a special frame of reference, σ_0. It is exactly that frame of reference in which the CMBR has no dipole due to the Doppler-effect [5]. This fact suggests the strong assumption that this frame of reference, σ_0, defines an absolute space in the sense of Newton. Therefore, a spherical, centrally point-symmetric light propagation is reasonably conceivable only in the frame of reference σ_0. Light propagates furthermore spherically and with speed c, but not further centrally symmetric with respect to the light source. From the perspective of the moving observer the center of the spherically shaped wave of light moves in reverse direction to the speed v of the moved frame of reference σ. Only an observer resting within the rest frame σ_0 observes a spherical wave front with its center at that position the light source had held at the moment of radiation.

The above derivation (Eq. 1.3) of the transformation formulas (Eq. 1.1 and Eq. 1.2) is, thus, obsolete. In addition, the postulate of the unchanged cross-dimensions loses its meaning, since only this postulate enables the close connection between length contraction and dilation of time.

In a series of papers, [6-11], we proposed a cosmological model, the CM, in which we use the frame of reference, σ_0, defined by the CMBR, in the sense of a special space-time. A 4-dimensional balloon with a thin 3-dimensional

envelope (membrane) expands in the 4D-hyperspace with an unknown speed of expansion, V_E. At the same time, a homogeneous vector field permeates the membrane perpendicularly. The membrane does not resist (or resists only marginally), if it is free of matter and tensed perpendicularly to the homogeneous vector field. However, when the membrane is charged with matter it resists. The resistance produces a force that causes the curvature of the membrane (curvature of space), and as an additional consequence, gravity and the effects of the dark matter.

One can illustrate the origin of the homogeneous vector field by different physical phenomena, for example a material flow reverse to the speed of expansion, V_E, or a material flow from the inside of the balloon, if one accepts over-pressure there. However, the origin of the homogeneous vector field can also be a form of radiation, or a completely new phenomenon. The authors hold back here, and enumerate here only some indispensables properties [8].

The following strong evidence speaks in support of the cosmic membrane model:

- The experimentally proven existence of the dipole-free frame of reference, σ_0. Therefore, the discovery of the CMBR by Wilson and Penzias [4] is one of the pillars of the CM.
- The result of the atomic-clock experiment of Häfele and Keating [3] can be explained much easier in the CM than in the SR. Therefore, the atomic-clock experiment is one of the key experiments of the CM.
- A 3D-membrane tensed in 4D-hyperspace bends under central load as 1/r, which corresponds exactly to Newton's gravitational potential. For this reason, gravity becomes simply a downhill force, and becomes clearly explainable [6].
- Another property of the membrane is that it clearly explains the decrease of the speed of light in a gravitational funnel, and it also explains in a simple manner light bending, radar echo delay, Einstein rings, and similar optical phenomena [8].
- Gravitational waves can appear in this cosmological model as well as longitudinal waves as in the form of transversal waves. The speed of the transversal waves still needs to be explicated.
- Another property of the curved membrane is the increased resistance. The increased resistance can explain the dark matter. Dark matter is, thus, a simple effect of the membrane which only arises together with the curvature of the membrane (curvature of the space), and therefore only in the neighborhood of real matter [7].
- The geodetic precession of a rotating body in the gravitational field can be explained by an increase in mass in the gravitational field together with the above mentioned change of the speed of light in the gravitational funnel [6].
- Frame-dragging is conceivable in the CM, but not the Lense-Thirring effect. We have shown [10] that the value of the Lense-Thirring effect found by the Gravity B Experiment is with high probability the geodetic precession of the gyroscopes in the gravitational field of the Sun, caused by the absolute speed in the rest frame σ_0. Therefore, the Gravity B Experiment is one of the key experiments of the CM.
- Because of the coefficient of elasticity of the membrane of $F_o=2.164\times10^{19}$ [N/m^2] [7], neutron stars of the mass of the Sun must have a diameter of at least 200 km. A similar restriction for the minimal size or maximal mass also holds for black holes.
- The fact that the electrons orbit the atomic nuclei without fatigue since the big bang, or that light waves propagate without fatigue over billions of years through the space, is probably the influence of the homogeneous vector field. The homogeneous vector field submits nonstop huge amounts of energy to the matter embedded in the membrane.
- Because of the extremely high coefficient of elasticity of the membrane of $F_o=2.164\times10^{19}$ [N/m^2] [7], one can conceive that the stuff the membrane is made of only as a glassy, super strong material (for comparison: steel has a coefficient of elasticity of about 2×10^{11} [N/m^2]). Therefore, it is more likely that waves propagate instead of particles [12].

The central, spherical propagation of light is explainable meaningfully only in the rest frame of reference, σ_0. Therefore, some questions arise concerning the SR. The classical derivation of the relativistic equations of the Lorentz-transformation, Eq. (1.1) and Eq. (1.2), is not valid anymore. It needs to be redone. In earlier work, we have published some results on this matter:

- Light propagates, as the CMBR does, only in the rest frame of reference σ_0. Far from centers of strong gravity, light propagates with constant speed *c*.
- Light paths remain constant independent of the inertial frame of reference if one uses, instead of the length contraction $l' = l\sqrt{1-\beta^2}$ according to Eq. (1.2), a new length contraction of the form $x' = x\left(1-\beta^2\right)$ together with a new cross contraction of the form $y' = y\sqrt{1-\beta^2}$ (a similar formula holds for *z'*).
- The above assumption of a new length and cross contraction causes a change of about ± 36 m/s of the measured speed of light according to the change in the speed of the Earth on its orbit around the Sun. However, here we had to use the old definition *v=s/t* (velocity is the quotient of distance *s* and time *t*). The distance *s* (covered in the rest frame of reference σ_0) remains constant in the CM, but the measurement of time *t* depends, with reference to the dilation of time, on the speed *v* of the clock in the absolute space σ_0, and on the strength of the gravitational field.
- There is no contradiction to the very exact measurements of the speed of light by Evenson et al. [13], because the speed of light is also constant under the paradigm of the membrane. An apparent contradiction arises only through the fact that Evenson and his team had replaced the distance *s* by the wave length *λ* of a source of reference. This way, the authors divide two frequencies and eliminate time dilation. This method corresponds to the assumption of an absolute time in the sense of Newton. (By the way, the series of the classical measurements of the speed of light ended in 1960 with errors of about ± 50 m/s [10]. Our prediction of a yearly variation of ± 36 m/s of the speed of light lies inside the error bar of the classic measurements.)
- The results of the experiments of Michelson-Morley and Kennedy-Thorndike constitute no proofs in support of or against one of the theories, because the null result is demanded by both theories, the SR and the CM. Actually, the Kennedy-Thorndike experiment would have to show a long-term effect, but this effect is not measurable by today's means according to our research.

In the present article, we show, that, under the paradigm of an absolute space, the Kennedy-Thorndike experiment would have to show a long-term effect. However, this effect is extremely small and undetectable by today's means. Moreover, the effect is not precisely defined because of the complicated interaction of the movement of the source of light in the absolute space and the red shift caused by gravity (see introduction).

The experiment of Kennedy and Thorndike [14] is an extension of the Michelson-Morley experiment as they use an interferometer with unequal arm length. Furthermore, the experiment has been planned as a long-term experiment for the purpose of studying the influence of the different directions of the movement of the Earth on its orbit around the Sun. The aim of the experiment by Kennedy and Thorndike has been to prove that the relativistic time dilation $t' = t/\sqrt{1-\beta^2}$ and the relativistic length-contraction $l' = l\sqrt{1-\beta^2}$ (with *β=v/c)* condition each other. In other words, only the Lorentz-transformation and, thus, the SR describe exactly the experiment. The null result should serve as proof, i.e., no change in the observed interference pattern during a rotation of the interferometer, and that based on an observation over a period of several months. Actually, Kennedy and Thorndike have found no change in the observed interference pattern, neither during rotation nor over the course of time. However, the accuracy of their experimental arrangement was low. In 1977, Mansouri and Sexl [15] criticized it, and suggested various improved tests, which have been performed later. In 1990, Hils and Hall and also Braxmaier [16,17] coupled a laser to an optical spectral line (line of reference), and to a second laser with a highly stable cavity. Based on the testing theory of Mansouri and Sexl, this experiment was 300 times more accurate than the original experiment of Kennedy and Thorndike. In 2004, Wolf et al. [18,19] used a cryogenic sapphire oscillator and a hydrogen maser. The frequency of the oscillator remained stable both during a rotation of the oscillator and over a long time, during which the Earth changed its speed orbiting the Sun (Kennedy-Thorndike test). The authors improved once more the accuracy of the experiment by a factor of 30. In 2009,

Tobar et al. [20] used a similar arrangement, and they further increased the accuracy. In 1995, Müller and Soffel [21], and in 1999, Müller et al. [22], performed an analysis of the data of the lunar laser ranging. They also found no evidence of a deviation of length-contraction and time dilation from the values demanded by the SR. The accuracy of their analysis was comparable with the results of Hils and Hall in 1990. So, all results of the newer experiments confirmed the result of Kennedy and Thorndike, i.e., the null effect.

However, already Robertson [23] had criticized in 1949 that the experiment of Kennedy and Thorndike only tests the ratio of length-contraction and cross-contraction. It is sufficient that the value of this ratio is that of the Lorentz factor $\sqrt{1-\beta^2}$. Exactly that is fulfilled as well in the CM and in the SR. Another criticism (by us) is the adherence to the long term stability of the source of light, more precisely the light's strength and frequency. We suggest a long term effect, but it is extremely small, and difficulties are very high to stabilize highly accurate interferometry during a period of several months. In addition, we comment that the modern laser technology obscures the effect (see Section 2).

We acknowledge in accordance with Michelson-Morley and Kennedy-Thorndike that no effect occurs during a rotation of the interferometer. This holds also when we use the length-contraction of the form $x' = x\left(1-\beta^2\right)$ together with an additional cross-contraction of the form $y' = y\sqrt{1-\beta^2}$ instead of the length-contraction $l' = l\sqrt{1-\beta^2}$ given by Lorentz. Otherwise, we contradict the null effect of time. The relativistic time dilation, $t' = t/\sqrt{1-\beta^2}$, which is experimentally well proven and used also by us, causes inevitably a small deviation or some other change in the interference pattern over the course of a year. The cause of the time dilation is the movement of the Earth around the Sun and its consequence in form of the change in the speed of the inertial frame *Earth* in the absolute space.

Monochromatic light is a requirement of interferometry. We will show that the production of monochromatic light, for example using an optical diffraction grating, does not depend on the orientation of the grating in each inertial frame, moved or resting. This statement also applies to the use of lasers. But we will also show that each change in the speed of the inertial frame causes a little change in the diffraction angle at the diffraction grating. The reasons for this are the change in the frequency of the light source caused by the relativistic time dilation $t' = t/\sqrt{1-\beta^2}$, and the involved change of the wavelength λ of the light.

In the following Section 1, we show, using the example of an optical grating, that a constant diffraction angle will be measured in each inertial frame of reference if one disregards the dilation of time. In Section 2, we show that the thermal broadening of the line width of the sources of light hides the long term effect of the Kennedy-Thorndike experiment. We also show that the use of lasers, cavities and Fabry-Pérot etalons do not change that either. In Section 3, we consider an oscillator model in an attempt to explain the relativistic dilation of time in connection with the increase of the relativistic mass. We discuss the results in Section 4, and in Section 5, we draw some conclusions.

2. DIFFRACTION OF LIGHT BY A GRATING IN MOVED INERTIAL FRAMES

In this section, we show using the example of a grating spectrograph that an optical arrangement would result in no effect caused by a change in the orientation in the space if one neglects the dilation of time. However, under consideration of time dilation, we find an error of the order of ± 3.6×10^{-08}. This value is extremely small, and, furthermore, it does not occur until after a period of three months. In Section 3, we show that this error is not detectable using today's means.

Grating spectrographs are widely used to measure the absolute wavelength of light and to find series of lines for identification of atoms or molecules. One disadvantage of grating spectrographs is the great loss of light by the slit. This disadvantage can be avoided by interference methods. The Fabry-Pérot spectroscopy, for example, is often used to investigate the fine structure of a single line [24], especially in astronomy. A good overview of the use of Fabry-Pérot spectroscopy in modern physics, astronomy and astrophysics is given by Lecian [25]. The reason, why we do not use the Fabry-Pérot spectrograph as an example, are simply the mathematical difficulties. The grating spectrograph is mathematically easier to handle.

The movement of an optical apparatus in the absolute space causes a series of changes and effects:

- A length-contraction and a cross-contraction depending on the orientation in the space and the speed of the movement.
- Connected with the length- and cross-contraction the angles of the moved coordinate axes can change.
- The light of a moving light source is subject to the Doppler-effect, i.e., the wave length depends on the direction of propagation.

The diffraction of light can be done by optical gratings. Optical gratings exist for a wide range of wavelengths – from microwaves to x-rays. The lattice constant *d* has to be of the order of the wavelength λ. In the case of visible light, one uses scratched transparent gratings made of glass (see Fig. 1). In the case of reflection, one can also use scratched metallic mirrors.

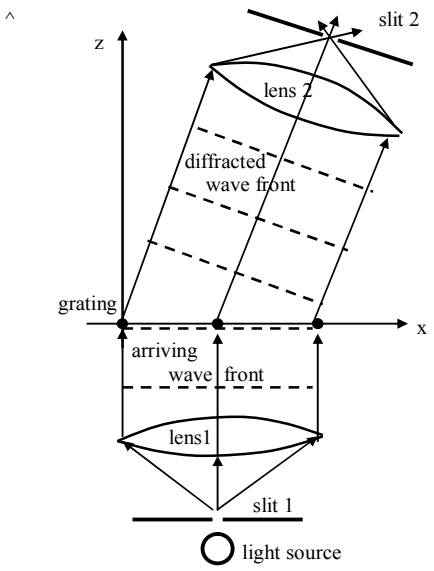

Fig. 1. Diffraction of a wave front by grating

We consider a certain wavelength λ_0, which should result from the diffraction arrangement as final product with the highest possible purity. A moving real light source produces the light. The light rays leave slit 1 in a divergent form. A lens collects the divergent rays and forms flat wave fronts. The flat wave fronts strike the optical grating. Behind the grating, the diffracted wave fronts are collected by a second lens to focus a band pattern. A second slit lets pass only light of about wavelength λ_0. This way, the optical arrangement produces nearly monochromatic light, which can be used for interferometric experiments.

The diffraction angle γ_k with respect to the x-axis is, for the k-th order diffraction maximum and wavelength λ_0,

$$\gamma_k = \arccos\left(\frac{k\,\lambda_0}{d}\right) \quad \text{with k = 0, 1, 2, ...} \qquad (2.1)$$

The main maximum for order k=0 is not interesting. It corresponds to the straight pass of the incoming wave front. We consider the first and strongest diffraction maximum for k=1 only. In this case, the diffraction angle is γ = arccos (λ_o / d).

We assume that the diffraction arrangement of Fig. 1 rests in the absolute space σ_0, i.e., its speed is v=0. The lattice constant is *d*, the wavelength λ_0, the x-z-coordinates of Slit 2 are $x=L_x$ and $z=L_z$, the diffraction angle is γ_1. The diffraction angle γ_1 is also the angle under which Slit 2 is seen from the origin of the coordinate system. Furthermore, we demand that the incoming wave fronts are exactly parallel to the x-axis, i.e., their normal vector $\vec{P}$ is arranged parallel to the z-axis.

Now we assume that the same diffraction arrangement moves with speed v>0 in an arbitrary direction $\vec{v}$ in the absolute space. The coordinate system (x', z') rests in the absolute space, but its origin is fixed at that point where the first wave front strikes point G_0 of the grating. The x'-axis is still parallel to the x-axis of σ_0, and the z'-axis is parallel to the z-axis of σ_0.

The Sun moves through the space in the direction of the Virgo cluster. The Earth orbits the Sun. The self-rotation of the Earth adds yet an additional speed component. Moreover, caused by the self-rotation of the Earth, an earth-bound laboratory changes permanently its orientation with respect to the course of the Sun. Therefore, we also consider the influence of the vector addition of velocities and the revolution of the local coordinate axes, coupled with the diffracting grating.

Around September 23rd (autumn point), the connecting line Earth-Sun is directed rather exactly to the Virgo cluster (constellation Virgo). We take the projection of this line on the ecliptic

(slice of Earth's orbit around the Sun) as x_E-axis of the long-term astronomically fixed coordinate system x_E, y_E, z_E. The z_E-axis is perpendicular to the ecliptic, and it is directed to about the north celestial pole. Then, the y_E-axis is directed to about the point the Earth is positioned on June 21. The axis of Earth has a declination of about 23° with respect to the z_E-axis, and it is directed exactly to the north celestial pole. We propose that the earthly laboratory together with the diffraction grating have the coordinates x_L, y_L, z_L. The x_L-axis is directed parallel to the longitudinal direction of the grating, i.e. perpendicular to the gridlines, the y_L-axis parallel to the gridlines, and the z_L-axis is vertically upwards-directed in the direction of the incident light beam of the source.

The axis of Earth is stable for a long time in the absolute space, and it is always declined by an angle of about 23° with respect to our z_E-axis in the direction of the $-y_E$-axis. This implies a rotation around the x_E-axis by 23°. However, the initial orientation of our earth's axis is parallel to the north celestial pole. We will align this axis later. The laboratory rotates together with its coordinate system x_L, y_L, z_L during the daily rotation of the Earth. Here, because of the small difference, we do not discriminate between sidereal time and solar time. We implement an initial orientation at autumn point (September 23). At this point, the axes x_L, y_L, z_L of the laboratory shall have the same directions as the axes x_E, y_E, z_E of the astronomically fixed ecliptic coordinate system. Additionally, we set the time to t=0. This corresponds to a laboratory site on the North Pole. Then, in a first step, we rotate the coordinate system x_L, y_L, z_L around the x_E-axis to get the declination of the needed degree of latitude, $\beta°$, this is where the laboratory is actually positioned. To simulate the daytime t corresponding to Earth's rotation, the second turn is performed around the z_E-axis by the angle ωt. The third and final turn is again about the axis z_E, so that Earth's axis gets the declination of 23° with respect to the z_E-axis in direction of the negative y_E-axis. We use the two rotation matrices:

$$D_x = \begin{pmatrix} 1 & 0 & 0 \\ 0 & \cos(\alpha) & -\sin(\alpha) \\ 0 & \sin(\alpha) & \cos(\alpha) \end{pmatrix} \tag{2.2}$$

and

$$D_Z = \begin{pmatrix} \cos(\alpha) & -\sin(\alpha) & 0 \\ \sin(\alpha) & \cos(\alpha) & 0 \\ 0 & 0 & 1 \end{pmatrix}. \tag{2.3}$$

Fig. 3 shows the constellation of Sun and Earth in the two coordinate systems.

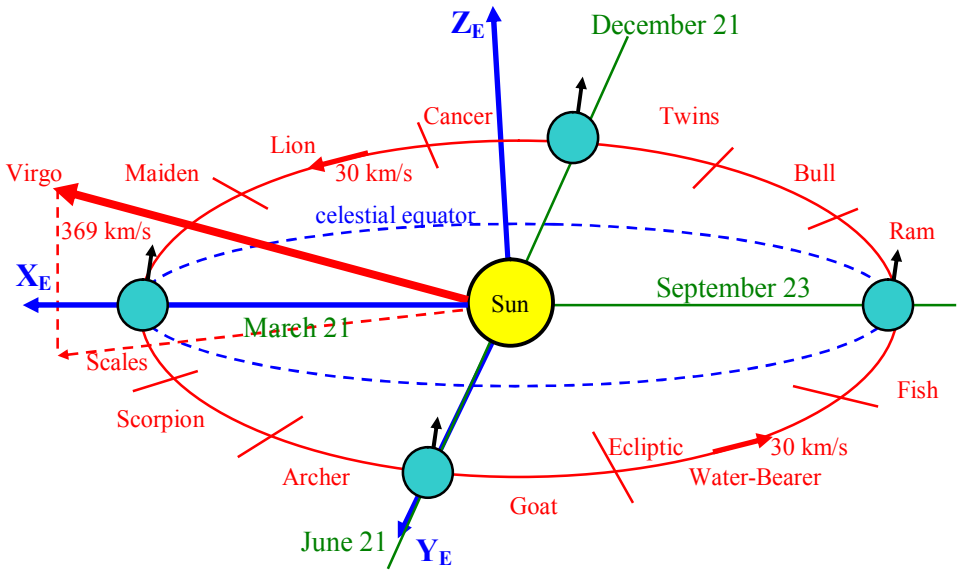

Fig. 2. The ecliptic coordinate system X_E, Y_E, Z_E

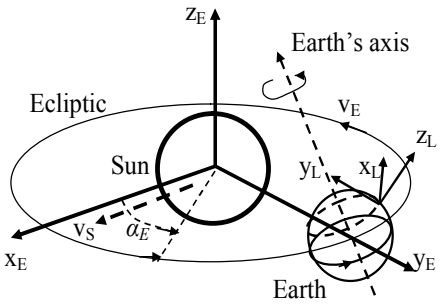

Fig. 3. The two coordinate systems – the ecliptic (E) and the laboratory (L)

Now, we assume that our diffraction grating (Fig. 1) moves with speed $\vec{v} = \vec{v}_S + \vec{v}_E + \vec{v}_R$ in the absolute space. Here, velocity v_S =369 km/s is the velocity oft he Sun in direction oft he Virgo cluster, velocity v_E is the velocity of the Earth on its orbit around the Sun with an orbital angle α_E with respect to the x_E-axis and an amount of 30 km/s, and velocity v_R is the velocity of the laboratory caused by the rotation of the Earth. In the not rotated coordinate system x_E, y_E, z_E, the three components of vector $\vec{v}$ are:

$$v_{xE} = 369 - 30\sin(\alpha_E) - v_{R0}\sin(\omega t), \quad (2.4)$$

$$v_{yE} = 30 \cdot \cos(\alpha_E) + v_{R0}\cos(\omega t)\cos(\alpha_A), \quad (2.5)$$

$$v_{zE} = \sin(\alpha_A)\, v_{R0}\cos(\omega t)\cos(\alpha_A). \quad (2.6)$$

Here, $v_{R0} = R_E\, \omega\, cos(\beta°)$, is the rotational speed in km/s with respect to the degree of latitude. The quantity R_E is the radius of Earth in km, the quantity ω is the angular frequency of Earth's rotation, the quantity α_E is the Earth's orbital angle as measured from the x_E-axis, the product ωt is the rotational angle of Earth's rotation measured from the x_E-axis, and the quantity α_A is the declination of Earth's axis as measured from the z_E-axis.

However, it is computationally easier to rotate the speed vector $\vec{v}$ the same three times, but with reverse angles, than to rotate the coordinate system of the laboratory x_L, y_L, z_L. The effect is identical. We compute the rotated vector $\vec{v}'$ by the following three consecutive turns as shown in Eq. (2.7).

$$\vec{v}' = D_{y,\alpha'}\left(D_{z,\omega t'}\left(D_{y,\beta'}\,\vec{v}\right)\right). \quad (2.7)$$

Because the laboratory has the initial position *North Pole*, we reach the needed degree of latitude, $\beta°$, by a rotation of $\pi-\beta$. However, because we had to take the reverse angle, we use here the rotational angle $\beta' = \beta-\pi$. In the case of the other two angles, ωt and α_A, a simple reversion of the sign is sufficient for proper orientation, i.e. $\alpha' = -\alpha_A$ and $\omega t' = -\omega t$.

We fix the coordinate system (x_L, y_L, z_L) in the absolute space σ_0 so that its origin O_L is positioned at that position of the grid point G_0 where the first wave front arrives at the middle of the grid line G_0. Fact is that the normal vector $\vec{P}$ of the wave fronts can also have an x_L-component as an y_L-component if we demand that the incoming light beam shall propagate parallel to the moving vertical of the grid. Therefore, we have to deal with two aberration angles, α_{xL} and α_{yL}, i.e., the planes of the wave fronts are sloped in two directions (Fig. 4 shows only the angle α_{xL}). This implies, we have to consider not only grid points but grid lines with some spatial extension in the y_L-direction. Grid point G_0 is the middle of grid line G_0, grid point G_1 is the middle of grid line G_1, etc. The wave fronts do not arrive simultaneously at all grid points G_0, G_1, ..., but consecutively. This holds also for the y_L-direction. In the case of an aberration in y_L-direction, the wave front does not hit simultaneously the whole line, but consecutively.

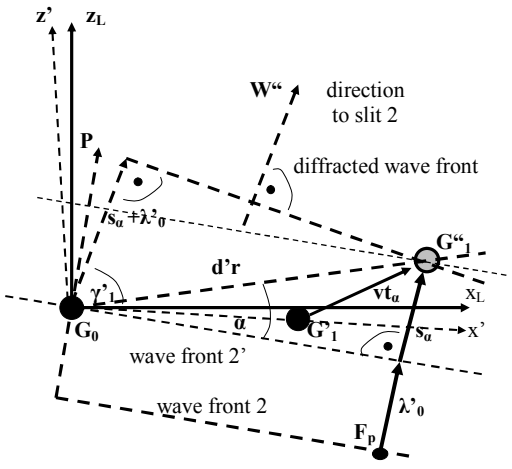

Fig. 4. Wave front and moving grid point G_1

A sphere in the absolute space σ_0 changes its shape if it is accelerated to speed $\vec{v}'$. This change in shape is caused by the fact that length contraction and cross contraction differ in magnitude. A sphere in the absolute space σ_0 is transformed into a spheroid or ellipsoid of rotation. The rotational axis is the minor axis, and it is parallel to the speed vector $\vec{v}'$. The two major axes are of the same length and perpendicular to each other. If none of the three axes of the coordinate system (x_L, y_L, z_L) is parallel to the speed vector $\vec{v}'$ (or anti-parallel) then the local axes shorten and twist. We obtain the magnitude and the new direction of the shortened and twisted x_L-axis by the following transformations. First, we compute the projection of $\vec{v}'$ onto the x-direction using the inner product. From the inner product we get the angle $\alpha_{v'x}$ between $\vec{v}'$ and the x-axis. (Remember that the axes x_L, y_L, z_L have the same directions as the axes x_E, y_E, z_E.) However, in the theory of the ellipse, the counting of the angles starts at the major axis. Therefore, we take as angle the supplement to the right angle, i.e.,

$$\alpha = \left|\pi/2 - \alpha_{v'x}\right| = \left|\pi/2 - \arccos(e_x \cdot e_{v'})\right| . \quad (2.8)$$

According to the theory of the ellipse the angle α changes into the angle α',

$$a' = \arctan((b/a)\tan(\alpha)) . \quad (2.9)$$

Here, $a = \sqrt{1 - v^2/c^2}$ and $b = 1 - v^2/c^2$ are the contracted axes of the unit circle. Then, we compute the unit vector $\vec{q}$ by a twofold application of the outer product. The unit vector $\vec{q}$ lies in the plane spanned by the vectors $\vec{e}_x$ and $\vec{e}_{v'}$. Simultaneously, the unit vector $\vec{q}$ is perpendicular to unit vector $\vec{e}_x$, i.e.,

$$\vec{q} = \left((\vec{e}_x \times \vec{e}_{v'}) \times \vec{e}_x\right) / \left|(\vec{e}_x \times \vec{e}_{v'}) \times \vec{e}_x\right| . \quad (2.10)$$

Now, we rotate the unit vector $\vec{e}_x$ by the angle $d_\alpha = \alpha' - \alpha$ and normalize it by way of

$$\vec{e}_{dx} = \frac{\vec{e}_x + d_\alpha \vec{q}}{\left|\vec{e}_x + d_\alpha \vec{q}\right|} . \quad (2.11)$$

We decompose the new unit vector $\vec{e}_{dx}$ and obtain its components *x* and *y*. Component *x* is the length of the length-contracted projection of vector $\vec{e}_{dx}$ onto vector $\vec{v}'$, and *y* the length of the perpendicular cross-contracted component.

$$x = a\cos(\alpha), \quad y = b\sin(\alpha). \quad (2.12)$$

We obtain the rotated and contracted vector $\vec{d}'_x$ (the original vector was $\vec{e}_x$) by Eq. (2.13). Vector $\vec{d}'_x$ is not an unit vector.

$$\vec{d}'_x = \vec{e}_{dx}\sqrt{x^2 + y^2} . \quad (2.13)$$

Similarly, we obtain the rotated unit vector $\vec{e}_{dz}$ and the rotated and contracted vector $\vec{d}'_z$. The y-direction of the laboratory plays a minor role in the computation of the diffraction angle. Therefore, there is no need of a transformation of the y-axis.

We turn to the construction of the normal vector $\vec{P}$ of the wave fronts. In the resting system, let the propagation of the light waves have exactly the direction of the z-axis. In the moving system the light beam has to propagate in parallel to the moving $\vec{z}'$-axis. After time *t*, the coordinates of the end point of vector $\vec{P}$ are

$$\vec{P}(t_z, t) = t_z\, c\, \vec{e}_{dz} + \vec{v}'\, t . \quad (2.14)$$

Here, *c* is he speed of light, and t_z a time that we compute so that for *t=1* the vector $\vec{P}$ has exactly norm *c*. Quantity t_z is computed iteratively.

Now, we compute the exact position of grid point G_1 for the moment at which it coincides with wave front 2. Grid point G_1 is positioned on the rotated and contracted axis $\vec{d}'_x$. Therefore, we term its position G'_1. During time $t_{\alpha\lambda'}$, grid point G'_1 has moved over the distance $\vec{v}'\, t_{\alpha\lambda'}$ to the new position G''_1 (see Fig. 4). Wave 2 has, during the same time, propagated, starting from the foot F_p, over the distance $\lambda'_0 + s_\alpha$. We find

$$\vec{G}''_1 = \vec{G}'_1 + \vec{v}'\, t_{\alpha\lambda'} \quad \text{with} \quad \vec{G}'_1 = d_0\, \vec{d}'_x \quad (2.15)$$

Distance s_α is the projection of vector $\vec{G}_1''$ onto the unit vector $\vec{e}_P$ (unit vector of the normal vector $\vec{P}$ of the wave fronts). We find

$$s_\alpha = \vec{e}_P \cdot \vec{G}_1'' \quad (2.16)$$

Time $t_{\alpha\lambda'}$ is computed iteratively so that the criterion (2.17):

$$(t_{\alpha\lambda'} - ((s_\alpha + \lambda'_0)/c))^2 = 0 \quad (2.17)$$

is fulfilled. This means, the distance from foot F_p to position G"$_1$ divided by speed of light *c* equals the runtime of grid point G_1 from position G'$_1$ to position G"$_1$. Here, wave length λ'_0 is wave length λ_0, but changed by the Doppler effect. By the motion of the light source through the space, a factor arises for wave length λ_0 of a resting source. This factor differs from value 1 by the projection of speed vector $\vec{v}'$ onto the direction of the normal vector $\vec{P}$, divided by the speed of light, *c*. Wave length λ_0 will, this way, either be shortened or lengthened.

$$\lambda'_0 = \lambda_0 \left(1 - \frac{\vec{v}' \cdot \vec{e}_P}{c}\right) . \quad (2.18)$$

Now, we calculate the direction $\vec{W}''$ of the diffracted beam. Vector $\vec{W}''$ has to fulfill the following three conditions: (1) the distance $s_\alpha + \lambda'_0$, starting from grid point G_0 and showing in direction of Slit 2, has to have exactly this amount; (2) and has to be exactly perpendicular to the connecting line G_0 - G"$_1$; (3) the outgoing beam has to lie at each moment *t* on the (x'-z')-plane. This plane moves with speed $\vec{v}'$ through the space. We set the components w_y and w_z of vector $\vec{W}''$ to:

$$w_y = v'_y t_{\alpha\lambda'} + \vec{e}_{dx,y} w_x + \vec{e}_{dz,y} \sqrt{(s_\alpha + \lambda'_0)^2 - w_x^2 - w_z^2} \quad (2.19)$$

and

$$w_z = \sqrt{(s_\alpha + \lambda'_0)^2 - w_x^2 - w_y^2} . \quad (2.20)$$

Component w_x has an arbitrary initial value between 0 and the grid constant d_0. Then, the exact value is computed iteratively so that the above three conditions are fulfilled. The quantities $\vec{e}_{dx,y}$ and $\vec{e}_{dz,y}$ are the y-components of the rotated unit vectors of the axes, $\vec{e}_{dx}$ and $\vec{e}_{dz}$. Equations (2.19) and (2.20) contain a vicious circle (circulus vitiosus), because we use in the Eq. (1.19) for the component w_y the component w_z which itself depends on w_y . However, one can leave the vicious circle by the use of a series expansion. One inserts preliminary values of w_z in the correcting term $\vec{e}_{dz,y} \sqrt{(s_\alpha + \lambda'_0)^2 - w_x^2 - w_z^2}$ of the w_y-component, and improves the value of w_z iteratively (interested readers can contact us). The above condition (2) is determined in the form of an inner product. The absolute value has to equal 0. The third condition, (3), is fulfilled automatically by Eq. (2.19). Therefore, the target criterion of the iteration of component w_x is:

$$(\vec{W}'' - \vec{G}_1'') \cdot \vec{W}'' = 0 . \quad (2.21)$$

Finally, we calculate unit vector $\vec{e}_{W''}$ from vector $\vec{W}''$.

Now, we consider the coordinates of slit 2. In the resting system σ_0, slit 2 is positioned at the distance *L* from the origin *O*. It is seen from this point under the angle γ_1, i.e., the coordinates of slit 2 are $L_x = L\cos(\gamma_1)$, $L_y = 0$ und $L_z = L \sin(\gamma_1)$. In the moved and rotated system σ', the coordinates L_x, L_y and L_z change by the length- and cross-contraction, depending on the length and the direction of the speed vector $\vec{v}'$. Therefore, we have to transform vector $\vec{L}$. We use the same method as we have used to transform the x- and the z-axis. First, we calculate the unit vector $\vec{e}_L$. Then, we calculate the inner product $\vec{e}_L \cdot \vec{e}_{v'}$, and, from this, the angle $\alpha_{v'L}$ between $\vec{L}$ and $\vec{v}'$, from angle α (see Eq. (2.8)). With angle α, we find the new angle α' due to the theory of the ellipse (see Eq. (2.9)), and with α' the angular difference $d_\alpha = \alpha' - \alpha$. With vector $\vec{q} = \left((\vec{e}_L \times \vec{e}_{v'}) \times \vec{e}_L\right) / \left|(\vec{e}_L \times \vec{e}_{v'}) \times \vec{e}_L\right|$, we construct an auxiliary unit vector in the plane of the vectors $\vec{L}$ und $\vec{v}'$, a vector that is also perpendicular to $\vec{L}$. We rotate unit vector $\vec{e}_{dL}$ by

the angle $d_\alpha = \alpha' - \alpha$, and normalize it in a similar way as given by Eq. (2.11). We obtain the rotated unit vector $\vec{e}_{dL}$. Now, we decompose the rotated unit vector $\vec{e}_{dL}$, and obtain its components *x* and *y*. Here, x is the length of the component that is parallel to $\vec{v}'$, and *y* the length of the perpendicular component. Component $x = a\cos(\alpha)$ is length-contracted, and component $y = b\sin(\alpha)$ is cross-contracted. From the two components, we obtain the contracted vector $\vec{l}_L'$, which is no longer a unit vector, i.e.,

$$\vec{l}_L' = \vec{e}_{dL}\sqrt{x^2 + y^2} \tag{2.22}$$

By normalization of vector $\vec{l}_L'$, we obtain the unit vector $\vec{e}_{dL}'$. Now, we have to model the motion of the whole arrangement of the origin and slit 2 with speed $\vec{v}'$ in absolute space. This method is similar to the construction of the wave normal $\vec{P}$. We find

$$\vec{e}_{dLvt}' = \vec{e}_{dL}' + \vec{v}'t_L . \tag{2.23}$$

Here, the quantity t_L is a time which is computed iteratively. The target criterion of the iteration is the equality of run time t_L of the arrangement in the space and run time of the wave front, i.e.

$$t_L = \left|\vec{e}_{dLvt}'\right| / c . \tag{2.24}$$

The unit vector $\vec{e}_{dLvt}'$ is the result of the iteration. In the last step, we calculate the two diffraction angles γ_{1L}' and γ_{1W}' of the moved arrangement from the two unit vectors $\vec{e}_{dL}'$ and $\vec{e}_{W''}$ as

$$\gamma_{1L}' = \arctan\left(\vec{e}_{dL,z}' / \vec{e}_{dL,x}'\right) \tag{2.25}$$

and

$$\gamma_{1W} = \arctan\left(\vec{e}_{W,z} / \vec{e}_{W,x}\right) . \tag{2.26}$$

Without consideration of a change in the wave length caused by the motion of the diffraction arrangement in the absolute space, the two angles are equal to each other (within computational accuracy), i.e.,

$$\gamma'_{1L} = \gamma_{1W} . \tag{2.27}$$

In y-direction, a residual error remains of magnitude $\varepsilon_y = 3 \times 10^{-10}$. However, this error is negligible because the grid lines are extended in y-direction by an amount that is much greater than this error. Probably, this residual error ε_y is caused by the finite series expansion of the vector component w_y (see Eq. (2.19)).

However, the results of our computations change dramatically with a change of the frequency of the light source due to time dilation, and the resulting change in the wave length from λ_0 to $\lambda_0' = \lambda_0 / \sqrt{1-\beta^2}$, i.e., depending on the speed $\vec{v}'$ of the arrangement in absolute space. A change in the diffraction angle ε_γ is connected with this change in the wave length, i.e.

$$\varepsilon_\gamma = \gamma_1'' - \gamma_1' . \tag{2.28}$$

Here, γ_1'' is the angle calculated after the relativistic change in the wave length due to the dilation of time.

In the following numerical example, the speed of light is $c = 3\times10^8$ m/s, wave length is $\lambda_0 = 5.6\times10^{-7}$ m, grid constant is $d_0 = 2\times10^{-6}$ m, the distance of slit 2 from the origin (grid point G_0) is L=0.3 m, the orbital speed of the Earth round the Sun is v_E = 30 km/s, and the speed of the Sun in the absolute space v_S = 369 km/s.

The mean change ε_γ in the diffraction angle is $\varepsilon_\gamma^{90} = 2.22\times10^{-7}$ for an angle of $\alpha_E = 90°$ of the orbit of the Earth. In the case in which the velocities of Sun and Earth add up, i.e., when $v = v_S + v_E$, $\varepsilon_\gamma = 2.58\times10^{-07}$. In the case of subtraction, we find $\varepsilon_\gamma = 1.86\times10^{-07}$. The mean value of $\varepsilon_\gamma^{90} = 2.22\times10^{-07}$ subtracts in Earth-bound diffraction experiments. So, only a relative angular deviation Δe_γ remains in the order of magnitude of $\Delta e_\gamma = \pm 3.6\times10^{-08}$ (see Fig. 5). This angular deviation is very small, and it does not appear until after three months. Fig. 5 shows the angular deviation $\Delta e_\gamma = e_\gamma - e_\gamma^{90}$ of the diffracted beam for one Earth's orbit around the Sun in units of 10^{-8} rad.

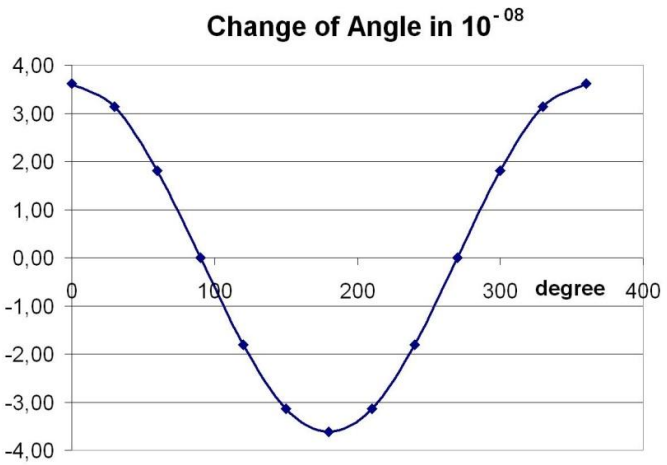

Fig. 5. Angular deviation Δe_γ of the diffracted beam over the angle of the Earth's orbit around the Sun

The Earth's self-rotation causes a much smaller effect compared with the effect of the Earth's orbit around the Sun. In our numerical example, we found an angular deviation of $e_\gamma = \pm 1.5 \times 10^{-10}$ rad per rotation.

3. LINEWIDTH AND LONG TERM STABILITY OF LIGHT SOURCES

In this section, we show that the long-term null-effect of the Kennedy-Thorndike experiment is incorrect with high probability. The Doppler effect caused by the thermal movement of the atoms in the active medium of the laser causes a finite line width of the laser light, and this line width masks the long-term effect predicted by us, and this masking is also not prevented by modern techniques as cryogenic cavities or Fabry-Pérot etalons.

A laser is basically a resonator (a tube) with concave mirrors at its ends (confocal resonator). The tube contains an active medium. The molecules or atoms of the medium have a sufficient number of energy levels. By the pumping of light energy from outside, a sufficient number of atoms or molecules get an excited state. First by spontaneous emission, light waves go back and forth. Then, by stimulated emission, the intensity of the light is amplified. One of the two mirrors is partially transparent. There, the usable coherent and only slightly divergent light beam emanates. This light is usable for the experiments.

The resonator amplifies several, closely spaced frequencies $v_0, v_1, ...$ The reason is the Doppler shift of the actual frequency of the atomic or molecular vibration in the medium. The frequencies $v_0, v_1, ...$ are subject to the resonator condition $v_i = n_k\ c/2L$, where n_k is an integer wavenumber, c the speed of light in the medium, and L the length of the light path between the two mirrors. However, the resonator does not amplify an arbitrary number of frequencies. The reason is that the envelope of the thermally caused line broadening has nearly a Gaussian shape (a Lorentzian function). The frequencies near the edge do not receive enough energy for the self-amplifying effect. One can select a single frequency v_0 by a Fabry-Pérot etalon. This etalon is a resonator with two partially transparent mirrors. A light beam can pass the Fabry-Pérot etalon only if it fulfills the resonator condition. The finesse F is the relation of that range around a resonance peak which is free from intensity and the width of the resonance peak. High-quality etalons reach F-values of $F = 10^6$.

Vaughan [24] gave in 1967 a good introduction to the construction and the use of Fabry-Pérot etalons in astronomy. One reason for its success is the high resolution and the small loss of intensity. A comparatively small Fabry-Pérot interferometer can outperform the largest gratings and reach a resolution suitable for the narrowest spectral lines. Hesser and Shawl [26] describe in 1977 the use of a single-etalon Fabry-Pérot interferometer for the use of ionized hydrogen in globular clusters. Lecian [25] lists, besides a review of modern developments in General Relativity, Cosmology and Quantum Gravity, a wide range of applications of the

Fabry-Pérot interferometer in particle physics, astronomy and astrophysics.

Generally, the Fabry-Pérot interferometer is used as a frequency standard, a tunable optical interference filter, or as laser resonator. If one wishes to scan a frequency band then the Fabry-Pérot etalon has to be tuned. Fine-tuning of the optical path length in etalon cavities is achieved by mechanical or piezo-electrical change of the distance between the two mirrors, or by slight variations of the cavity's index of refraction. Such index of refraction variations are accomplished by varying the relative gas mixture in gas-gap etalons or UV-exposing doped glass layer(s) in solid etalons. Another method, for example, is the use of a liquid crystal cavity tuning element [27].

The linewidth Δv is the width of that range of the frequency interval that is occupied by a single line of the frequency spectrum. The linewidth is defined by the half-width of the peak, i.e. its width at the half height. One assumes as causes the general energy uncertainty of Heisenberg (resonance curve, Lorentzian function), and, in addition, the Doppler effect caused by the thermal vibrations of the emitting atoms or molecules. The course of the intensity, $I(v)$, over the frequency v is similar to a Gaussian function (bell curve) with its maximum at frequency v_0. For example, the H_α-line of the Balmer series of hydrogen with λ=656.4 nm has a thermal line broadening of $\Delta\lambda$= 0.0036 nm at the temperature of 60 K, and at the temperature of 6000 K a thermal line broadening of $\Delta\lambda$= 0.036nm. The natural line width for the Hα-line is $\Delta\lambda \sim 2\times10^{-5}$ nm.

The Schawlow-Townes-limit defines the lower limit of the linewidth of the light of a laser. However, the Schawlow-Townes-limit is very small. Only extremely faint solid state lasers hit the limit. This type of laser works at temperatures near the absolute zero. The causes of the finite linewidth include spontaneous emission which is not in phase, Heisenberg's relation of energy uncertainty, and interactions of the photons with the components of the laser causing noise [28]. In the case of gas lasers, but also solid state lasers not working in the cryogenic temperature range, one has to add inevitably to the linewidth the Doppler effect of the moving atoms. The pumping power of a laser has to be at least the tenfold of the radiation power. This fact causes an input of energy that does not simplify temperature stabilization. In the same way, one gets a smaller aperture of the produced beam only by a higher pumping power. The aperture is inversely proportional to the coherence length.

Currently, the LIGO-observatories (Laser Interferometer Gravitational-wave Observatory) use that type of interferometers with the highest coherence length of the used monochromatic light, for example in Hanford (USA, Washington) or Livingston (USA, Louisiana). Several times, observatories of this kind have detected gravitational waves [29,30,31]. The observatories use a Michelson-interferometer with an arm length of 4 km in Livingston (2 km in Hanford). However, the effective arm length is about 1120 km by multiple mirroring. The mirrors are so adjusted that both partial rays erase one another by interference. The passage of a gravitational wave changes the lengths of the light paths in a different way. The partial rays do not erase one another any more, and a photodiode sends a signal.

The CM allows gravitational waves in two forms – longitudinal and transversal. However, one cannot use arbitrary weak solid state lasers working in the cryogenic temperature range, because the frequencies of the gravitational waves are in the audio band, and this sort of lasers is unable to record the quick change in the signal. In the practice of the detection of gravitational waves, a laser is used with a light power of 20 W laser output. Additionally, one has to handle noise and errors, for example the temperature control of the laser, the temperature control of the long tunnel tubes of the arms, or seismic vibrations. The interferometer registers even the fine vibrations of the ocean surf at a distance of several hundred miles. That is the reason why one has permanently to perform corrections, mostly through piezo-electrically changeable mirror positions. Thus, a long term effect is hidden behind a great number of corrections.

Another issue is the stabilization of frequency. The frequency of the emitted light of the laser is subject to fluctuations. Reasons and causes are manifold, for example fluctuations of the temperature or pressure of the medium, thermal expansion of the tube, fluctuations of the pumping power, and, additionally by our theory, a seasonal fluctuation of the frequencies of atomic transitions.

Stabilization with optical resonators is one of the common methods today. A resonator is

constructed using a stable tube and two mirrors at the ends in a constant distance, similarly to the construction of the laser. One of the mirrors is transparent to a small percentage. Before the light waves leave the resonator through the transparent mirror, they run several times back and forth between the two mirrors. Hereby, the constancy of the distance between the mirrors is very important. Therefore, one uses silicon for the tube in the cryogenic temperature range. This way, one avoids thermal noise to a large extent, and one achieves a line width of some few mHz with the resonator [32]. In the CM, the length of the optical path between two mirrors does not change with the speed of motion in the absolute space [10]. The light path remains absolutely constant by the interaction of length- and cross-contraction. Such an optical resonator, manufactured from silicon and running in the cryogenic temperature range is indeed a stable frequency standard.

However, we posit that a laser with frequency v_0 stabilized by such a resonator will react only by a tiny change of its light power to a general change in the frequencies caused by the dilation of time. The reason is that the medium of the laser produces light with a line width much greater than the line width of the frequency normal. The frequencies v_0, v_1, ... of the laser modes do not change due to CM, because they are a feature of the laser resonator. These frequencies are assigned to the maxima of the intensity function $I(v)$ over the frequency v. Also, the frequency v_0 of an etalon does not change. A frequency fluctuation of the atomic transitions in the laser just moves the center of mass of the envelope of Gaussian shape. In Fig. 6, the dashed line shows a second intensity function $I(v)$ due to a small left shift of the Gaussian curve. One can see that the intensity of the frequency of the etalon, i.e. $I(v_0)$, changes only negligibly. However, the intensities of the modes besides the main maximum at v_0 change more clearly.

The wave length (the frequency v_0) does not change either at the output of the laser or the output of a Fabry-Pérot etalon, but a small change of the light power is possible. This implies that a long term effect caused by the dilation of time does not cause a change in the interference pattern, but only a minimal fluctuation of the brightness over the course of a year. In addition, we have to add to this the previously unexplained influence of the relativistic change of mass and the relativistic contraction of the Earth on the gravitational field, and, thus, to the gravitational red shift of the frequency lines.

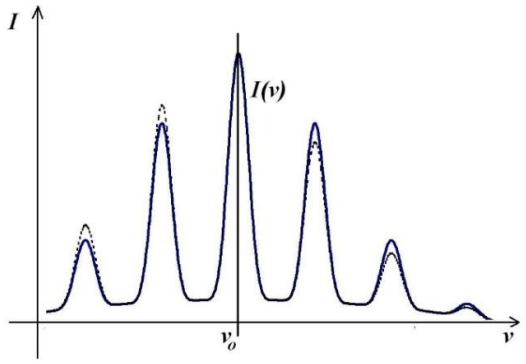

Fig. 6. Change in intensity of the laser modes by line shift

4. DILATION OF TIME UNDER THE PARADIGM OF A MEMBRANE

Einstein's general relativity theory and CM conform to each other to 88%, SR and CM conform to 93% [9]. This implies that small differences exist between the theories. According to our statements in the introduction (Section 1, Eq. (1.3)), it is most likely that the dilation of time is not coupled with the length-contraction. In this section, we show that the probability is much greater that a connection exists between the dilation of time and the relativistic increase of mass. Both phenomena, the dilation of time and the relativistic increase of mass, are experimentally well proven facts.

The dilation of time is dependent on the speed $\vec{v}$ of the clock

$$t' = t / \sqrt{1-\beta^2}\ , \qquad \text{(see Eq. (1.1)).}$$

For the relativistic increase of the transverse mass Eq. (4.1) is generally accepted [27].

$$m(v) = m_0 / \sqrt{1-\beta^2}\ . \tag{4.1}$$

We have derived this from the energy square [9] in coincidence with Puthoff [33]. Until now, we have not found a specific theory in the context of the CM for both phenomena – neither for the dilation of time nor the relativistic increase of mass. Therefore, we use, for the time being, Eq. (1.1) and Eq. (4.1) as experimentally well proven

phenomena. Here, in both formulae, $\beta=v/c$ and $\vec{v}$ the speed in the absolute space.

To connect the dilation of time with the relativistic increase of mass consider a harmonic undamped oscillator. The oscillator is constructed using two oscillating masses *m*, swinging against each other, and connected by an ideally elastic spring with spring constant k.

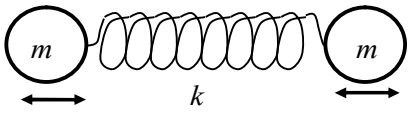

Fig. 7. Harmonic oscillator

The homogeneous ordinary differential equation of the oscillator is, at rest, in the absolute space:

$$m_0\,\ddot{x}(t)+k_0\,x(t)=0 \quad . \tag{4.2}$$

The quantity m_0 is the oscillating mass, quantity k_0 is the spring constant. The natural frequency ω_0 is

$$\omega_0=\sqrt{\frac{k_0}{m_0}} \quad . \tag{4.3}$$

Now, suppose the same oscillator is in motion. The dilation of time (or the decrease of frequency) caused by the relativistic increase of mass due to Eq. (4.1) is given by Eq. (4.4) for the case in which the harmonic oscillator oscillates perpendicularly to speed $\vec{v}$.

$$\omega(v)=\sqrt{\frac{k(v)}{m(v)}}=\sqrt{\frac{k(v)}{m_0}\sqrt{1-\beta^2}} \quad . \tag{4.4}$$

However, the desired result for the change in frequency, $\omega(v)=\omega_0\sqrt{1-\beta^2}$, demands that we accept the relation given in Eq. (4.5) for the dependency *k(v)*, i.e.,

$$k(v)=k_0\sqrt{1-\beta^2} \tag{4.5}$$

Indeed, from this follows:

$$\omega(v)=\sqrt{\frac{k_0}{m_0}\left(\sqrt{1-\beta^2}\right)^2}=\omega_0\sqrt{1-\beta^2} \quad . \tag{4.6}$$

But what does Eq. (4.5) mean? The transversal constant of elasticity of the harmonic oscillator decreases with increasing speed $\vec{v}$ in the absolute space. We have yet to find an appropriate model that would explain this relation. We will focus our future research on this topic. Equation (4.5) also says, indirectly, that particles could be more fragile at high speed than at rest. Despite intensive search, we have not found any evidence in support of this proposition [34-36].

5. RESULTS AND DISCUSSION

The SR posits the null effect in the case of the Michelson-Morley experiment. In the case of the Kennedy-Thorndike experiment, the SR demands, in addition, the null effect for a long term period of time. The CM also demands the null effect for both the Michelson-Morley experiment and for the Kennedy-Thorndike experiment in the case of short term experiments. However, in the case of the Kennedy-Thorndike experiment, the CM predicts a long term effect (after three months) in the order of 10^{-8} of the diffraction angle. The reason of this long term effect is the change in frequency of the moved light source caused by the dilation of time, and this is triggered by the change in the Earth's speed in the absolute space (see Section 2). However, the Earth's gravitational field remains as the big unknown (see introduction).

However, given today's means, one can not measure a diffraction effect in the order of 10^{-8}. Therefore, the long term effect remains hidden. In the CM, light paths are constant and do not dependent on the speed and the orientation of the optical arrangement in the absolute space. Therefore, all effects come from the dilation of time. The long term effect caused by the dilation of time has only a small impact on the intensity of a laser-based interferometer as was shown in Section 3. However, an experiment without the use of a Fabry-Pérot etalon would also fail because the natural line width of the laser is broadened by the thermal Doppler effect, and, for this reason, significantly greater than the effect under scrutiny (10^{-6} compared to 10^{-8}).

Müller et al. [21,22] had analyzed the data of the Lunar Laser Ranging, and confirmed the null effect over a period of some years. We have no explanation of this result, but we refer to a similar discussion related on the LAGEOS mission [9, 37,38,39] in the context of the Lense-Thirring effect. The interaction of the motion of the

satellite with the gravitational field and relativistic effects seems to involve some riddles which we are unable to explain, until now. The explanation becomes even more complicated when one considers that the system *Earth-Moon* could be subject to the dilation of time in a way similar to the orbitals of the system *atomic nucleus* – electrons which are subject to the dilation of time.

A clock t_0 indicates Newton's absolute time if it is resting in the absolute space and far away from gravitational fields. The CM says that the absolute time t_0 only depends on the speed of the expansion, V_E, of the cosmic membrane. However, a clock in motion works with a decelerated time interval t as indicated by Eq. (1.1). One needs to compute the integral Eq. (5.1) in all cases in which the speed of motion changes.

$$t_0 = \int_0^T \frac{d\tau}{\sqrt{1-\left(v(\tau)/c\right)^2}} \qquad (5.1)$$

The integral adds the changing time intervals depending on the changing speed of the clock. All earth-bound clocks are subject to this change in motion over the course of a year. Fig. 8 illustrates the annual relative frequency shift $\Delta\nu = \nu_S - \nu_E$, caused by the dilation of time, between a clock that moves with the Sun and a second clock that moves with the Earth.

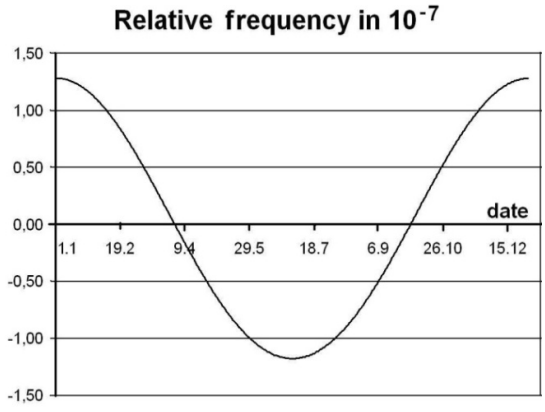

Fig. 8. Relative frequency in 10^{-7}

The dilation of time adds to the difference of time, t_S-t, between sun-time t_S and the time indicated by an earthbound clock t as shown in Fig. 9.

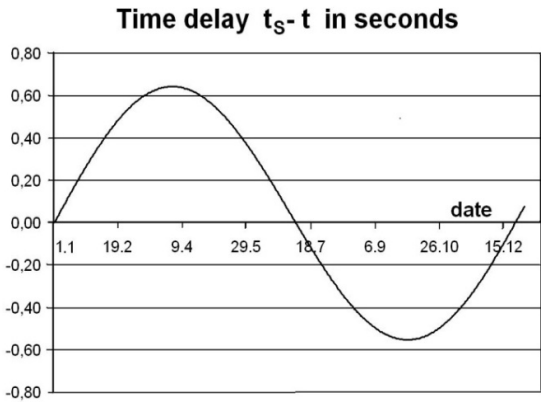

Fig. 9. Time delay $t_S - t$ in seconds

After the course of a year, a small time difference remains between the two clocks of about Δt=0.08 seconds. The reason is that the Sun moves straightly whereas the Earth orbits additionally the Sun. However, both clocks run more slowly than a resting clock, t_0. The time difference Δt between the time indicated by a resting clock t_0 and sun-time t_S is $\Delta t = t_0 - t_S = 23.87$ seconds after one year, calculated with a speed of v_S=369 km/s of the Sun in the absolute space.

The Häfele-Keating experiment [3] used six atomic clocks. One pair of these clocks traveled with normal passenger jets eastwards, another pair westwards around the globe. The third pair remained in the institute for comparison. The first pair of the clocks traveled with the self-rotation of the Earth, the second pair against. So, over the course of two days, the first pair orbited the Earth three times (1.5 ω with ω as angular frequency of Earth's rotation), but the second pair only once (0.5 ω). Because jets move in an altitude of about 30.000 feet, the gravitational force of the Earth is diminished and speeds up the clocks. Here, we do not discuss this effect, because it is not interesting in this consideration. We consider only the effect of the time dilation caused by the motion of the clocks. For further simplification, we assume that all speed vectors lie in the ecliptic, i.e., in the x-y-plane (see Fig. 2). Because the center of Earth does not change significantly its speed and its direction in the absolute space during two days, the movement of both pairs of clocks can be described by Eq. 5.2.

$$\vec{v} = \begin{pmatrix} v_{Ex} \\ v_{Ey} \end{pmatrix} + v_R \begin{pmatrix} \cos(k_i \omega t) \\ \sin(k_i \omega t) \end{pmatrix} \quad \text{with } i = 1, 2 \qquad (5.2)$$

Here, the quantity v_E is the nearly-constant short-time speed of the Earth in the absolute space, the quantity v_R is the rotational speed of the clocks with $v_R = R_E\, k_i\, \omega\, cos(\beta°)$ (see Eqs. 2.5 and 2.6), and k_1=1.5, k_2=0.5. For the integration of Eq. 5.1, one has to calculate the square of speed vector $\vec{v}$. We obtain:

$$v^2 = v_{Ex}^2 + 2v_{Ex}v_R\cos(k_i\omega t) + v_R^2\cos^2(k_i\omega t) + v_{Ey}^2 + 2v_{Ey}v_R\sin(k_i\omega t) + v_R^2\sin^2(k_i\omega t) \quad (5.3)$$

The integrand of integral 5.1 has an absolute value near one, i.e., 1-ε. So we can replace the root-function $\sqrt{1-\varepsilon}$ by 1-ε/2, and, in the division, replace by the change of the sign, i.e., 1+ε/2. Integrating over full days, the mixed terms, containing the sine- and cosine-function, disappear. The comparison of the clocks implies subtraction of the calculated values of the two integrals. Here, during subtraction, the constant term v_E^2 disappears as well. The remaining part describes the Häfele-Keating result, and this is the same result as found by the SR (after some discussions concerning relativity and inertial frames). Because the comparison of clocks needs the direct contact, only motions with full circles are allowed, and, this way, the influence of the absolute space disappears. In the CM, one needs no discussion of relativity to explain the Häfele-Keating result. Therefore, the atomic-clock experiment is one of the key experiments of the CM.

Earth-bound clocks are subject to various influences, for example the gravitational field of the Earth. But the main effect comes from the change in speed of the clock in absolute space (see introduction). This effect acts also in the case of atomic clocks. Atomic clocks do not indicate the absolute time t_0 but the time given by the integral Eq. (5.1), and that regardless of the increasing precision of the clock (cesium clock, rubidium fountain clock). The reason is that the two types of clocks use the frequency of atomic transitions between energy levels. The frequency of the actual clock, a quartz watch, is controlled by the atomic frequency, and so also subject to the dilation of time [40].

A light clock of special construction perhaps could indicate Newton's absolute time t_0 nearly precisely. In the CM the light path remains constant between two fixed mirrors independently of speed and orientation in space [10]. Therefore, a Fabry-Pérot etalon will not change its frequency pattern, also if speed and orientation changes. A cryogenic frequency standard with a precision of a few mHz [26] combined with a frequency comb [41] are a promising approach. The frequency comb delivers the desired frequency, whereas the Fabry-Pérot etalon secures the stability. With other words, one needs to select a constant wave length at the output of the laser of the frequency comb by the use of a Fabry-Pérot etalon. The frequency of light is too high to use it as input for a digital counter. One needs a second clock of the same construction, but with a slightly changed frequency. Then, by interference between the output beams of the two clocks, one obtains a countable signal. This type of clock avoids the influence of the dilation of time which controls the atomic sources of the laser light. Otherwise, the line width of the atomic source inside the laser should not be smaller than the annual change in frequency. This condition ensures that the cryogenic frequency standard and the frequency comb are supplied with light energy throughout the year. One of the remaining sources of errors is the acceleration and rotation of the cryogenic frequency standard caused by the motion of the Earth and its rotation. Based on Einstein's results [42], acceleration has the same effect as gravitation. Rotation also changes the frequency as the experiment of Sagnac [43] has shown. Another question is: Does it make sense, Newton's absolute time? It is correct only for a point without gravity and without any movement in absolute space.

Possibly, one could explain the dilation of time by an oscillator model. The increase of the relativistic mass together with a relativistic decrease of the constant of elasticity could possibly decrease the oscillator frequency. Unfortunately, we have yet to find adequate models that could explain the relativistic decrease of the constant of elasticity and the relativistic mass by the means of the membrane. However, we consider this paper as another introduction to the physical explanation of basic phenomena [44,45]. Using the time and the dilation of time, we try to leave the pure mathematical description of the phenomenon as given by Eq. (1.1), and to obtain a more fundamental statement that might, someday, be derived from the properties of the cosmic membrane themselves.

6. CONCLUSIONS

Accepting Newton's absolute space, the derivation of the dilation of time in the sense of the SR, i.e. together with the derivation of the length contraction under the constraint of constant cross dimensions, loses its plausibility. One has to go other ways to explain the experimentally well proven dilation of time with the help of the physical properties of the space.

The difficulties are enormous since, up to now, the unification of the quantum theory and the theory of gravitation does not exist. Additional important questions arise, beginning with the nature of the dark matter, and ending with the question, what space and time actually constitute. Therefore, we will concentrate our efforts on the search of proper models, which could become a little step in the pursuit of truth.

COMPETING INTERESTS

Authors have declared that no competing interests exist.

REFERENCES

1. Ives HE, Stilwell GR. An experimental study of the rate of a moving atomic clock. J. Opt. Soc. Am. 1938;28:215-226.
   Available:https://www.researchgate.net/publication/249333957_An_Experimental_Study_of_the_Rate_of_a_Moving_Atomic_Clock
2. Botermann B, et al. Test of Time Dilation Using Stored Li+ Ions as clocks at relativistic speed. Phys. Rev. Lett. 2014;113:120405.
   Available: Test of Time Dilation Using Stored Li+
3. Häfele JC, Keating R. Around-the-world atomic clocks: Predicted relativistic time gains. Science. 1972;177:166-170.
   Available:http://www.sciencemag.org/content/177/4044/168.abstract
4. Penzias AA, Wilson RW. A measurement of excess antenna temperature at 4080 Mc/s. ApJ. 1965;142:419-421.
   Available:http://dx.doi.org/10.1086/148307
5. Kogut A, et al. Dipole Anisotropy in the COBE Differential Microwave Radiometers First-Year Sky Maps. Astrophys. J. 1993; 419:1–6.
   Available:http://arxiv.org/abs/astro-ph/9312056
6. Von Weber S, Von Eye A. Multiple Weighted Regression Analysis of the Curvature of a 3D Brane in a 4D Bulk Space under a Homogeneous Vector Field. InterStat; 2010.
   Available:http://interstat.statjournals.net/YEAR/2010/articles/1007003.pdf
7. Von Weber S, Von Eye A. Monte Carlo study of vector field-induced dark matter in a spiral galaxy. InterStat; 2011.
   Available:http://interstat.statjournals.net/YEAR/2011/articles/1108002.pdf
8. Von Weber S, Von Eye A. Error analysis of simulated Einstein rings under the membrane paradigm. InterStat; 2013.
   Available:http://interstat.statjournals.net/YEAR/2013/articles/1310001.pdf
9. Von Weber S, Von Eye A. Geodetic precession under the paradigm of a cosmic membrane. Phys. Sci. Int. J. 2016; 10(4):1-14.
   Available:http://www.sciencedomain.org/abstract/14928
10. Von Weber S, Von Eye A. Two-way and one-way vacuum speed of light under the membrane paradigm. Phys. Sci. Int. J. 2017;15(2):1-17.
    Available:http:Two-way and One-way Vacuum Speed of Light under the Membrane ...
11. Onoochin V, Von Weber S. On the size of moving rigid bodies determined from conditions of equilibrium of ions in a crystalline lattice. In Einstein and Poincaré: The Physical Vacuum. Dvoeglazov VV, editor. Apeiron Montreal; 2006.
    ISBN: 0-9732911-3-3
    Available:Einstein and Poincare: the physical vacuum - PDF Free Download
12. Mueller E. De la réalité des nombres, Bull. Soc. Frib. Sc. Nat. 2014;103:83-90.
    Available:https:De la réalité des nombres - e-periodica
13. Evenson KM, et al. Speed of light from direct frequency and wavelength measurements of the methane-stabilized laser. Phys. Rev. Lett. 1972;29(19):1346-49.
    Available:https://dx.doi.org/10.1103%2FPhysRevLett.29.1346
14. Kennedy RJ, Thorndike EM. Experimental establishment of the relativity of time. In: Physical Review. 1932;42(Nr. 3):S.400–418.

Available:bibcode:1932PhRv...42..400K.
doi:10.1103/PhysRev.42.400

15. Mansouri R, Sexl RU. A test theory of special relativity. I: Simultaneity and clock synchronization. General Relat. Gravit. 1977;8(7):497-513.
DOI: 10.1007/BF00762635
16. Hils D, Hall, JL. Improved Kennedy-Thorndike experiment to test special relativity. In: Phys. Rev. Lett. 1990;64(Nr. 15):S.1697–1700.
Available:bibcode:1990PhRvL..64.1697H.
doi:10.1103/PhysRevLett.64.1697
PMID 10041466.
17. Braxmaier C, et al. Tests of relativity using a cryogenic optical resonator. In: Phys. Rev. Lett. 2002;88(Nr. 1):S.010401.
Available:bibcode:2002PhRvL..88a0401B.
doi:10.1103/PhysRevLett.88.010401
PMID: 11800924.
18. Wolf, et al. Tests of Lorentz invariance using a microwave resonator. In: Physical Review Letters. 2003;90(Nr. 6):S.060402.
Available:arxiv:gr-qc/0210049.
bibcode:2003PhRvL..90f0402W.
doi:10.1103/PhysRevLett.90.060402
PMID: 12633279.
19. Wolf, et al. Whispering gallery resonators and tests of Lorentz invariance. In: General Relativity and Gravitation. 2004;36(Nr. 10):S.2351–2372.
arxiv:gr-qc/0401017.
bibcode:2004GReGr..36.2351W.
doi:10.1023/B:GERG.0000046188.87741.51
20. Tobar, et al. Testing local Lorentz and position invariance and variation of fundamental constants by searching the derivative of the comparison frequency between a cryogenic sapphire oscillator and hydrogen maser. In: Physical Review D. 2010;81(Nr. 2):S.022003.
Available:arxiv:0912.2803.
bibcode:2010PhRvD..81b2003T
DOI: 10.1103/PhysRevD.81.022003
21. Müller J, Soffel, MH. A Kennedy-Thorndike experiment using LLR data. In: Physics Letters A. 1995;198:S.71-73.
DOI: 10.1016/0375-9601(94)01001-B
22. Müller, et al. Improved Determination of Relativistic Quantities from LLR. In: Proceedings of the 11th International Workshop on Laser Ranging Instrumentation. 1999;10:S.216-222.
Available:http:Improved Determination of Relativistic Quantities from LLR
23. Robertson HP. Postulate versus observation in the special theory of relativity. In: Reviews of Modern Physics. 1949;21(Nr.3):S.378-382.
Available:https:10.1103/RevModPhys.21.378
24. vaughan AH. Astronomical Fabry-Pérot interference spectroscopy. Ann. Rev. Astron. Astrophys. 1967;5:139-166.
Available:Astronomical Fabry-Perot Interference Spectroscopy - SAO/NASA ADS
25. Lecian OM. Alternative uses for quantum systems and devices. Symmetry. 2019; 11(4):462.
DOI: 10.3390/sym11040462
Available:(PDF) Alternative Uses for Quantum Systems and Devices | Orchidea ...
26. Hesser JE, Shawl SJ. An optical search for ionized hydrogen in globular clusters. 2. Astrophys. J. 1977;217:L143-L147.
Available:An optical search for ionized hydrogen in globular clusters. II
27. Ru-Pin Pan, et al. A novel tunable diode laser with liquid crystal intracavity tuning element.
Available:https://doi.org/10.1080/15421400490439194
28. Schawlow AL, Townes CH. Infrared and Optical Masers, Phys. Rev. 1958;112: 1949-1949.
Available:https: Infrared and Optical Masers
29. Abbott, et al. GW170817: Observation of Gravitational Waves from a Binary Neutron Star inispiral, Phys. Rev. Lett., Band. 2017;119.
Available:https:GW170817: Observation of Gravitational Waves from a Binary Neutron ...
30. Abramovici, et al. LIGO: The laser interferometer gravitational-wave observatory. Science. 1992;256:325-333.
Available:https:LIGO: The Laser Interferometer Gravitational-Wave ... - Science
31. Kessler, et al. A sub-40-mHz-linewidth laser based on a silicon single-crystal optical cavity. Nat. Photonics, Online 9. September 2012.
Available:https:A sub-40-mHz-linewidth laser based on a silicon single-crystal optical ...
32. Joos G. Theoretical physics. 15th Edition. AULA-Verlag Wiesbaden; 1989. German.

33. Puthoff HE. Polarizable-Vacuum approach to GR. Found. of Physics. 2002;32(6):1-24. Available:https://arxiv.org/ftp/gr-qc/papers/9909/9909037.pdf
34. Shiltsev VD. High energy particle colliders: Past 20 years, next 20 years and beyond. Fermilab Accelerator Physics Center; 2013. Available:https:HIGH ENERGY PARTICLE COLLIDERS: PAST 20 YEARS, NEXT 20 ...
35. Ruggiero F. Theoretical aspects of some collective instabilities in high-energy particle storage rings, CERN European Organization for Nuclear Research; 1986. Available:http:theoretical aspects of some collective instabilities in high-energy ...
36. Heidbrink WW. Basic physics of Alfvén instabilities driven by energetic particles in toroidally confined plasmas .... Physics of Plasmas. 2008;15:055501. Available:https:Basic physics of Alfvén instabilities driven by energetic particles in ...
37. Ciufolini I. Dragging of inertial frames. Nature. 2007;449:41-47. Available:http://www.nature.com/nature/journal/v449/n7158/abs/nature06071.html
38. Ciufolini, et al. A test of general relativity using the LARES and LAGEOS satellites and a GRACE Earth gravity model: Measurement of Earth's dragging of inertial frames. Eur Phys J C Part Fields. 2016; 76(3):120. DOI: 10.1140/epjc/s10052-016-3961-8. Epub 2016 Mar 4. Available:https://www.ncbi.nlm.nih.gov/pmc/articles/PMC4946852/
39. Nordtvedt K. Lunar laser ranging - a comprehensive probe of Post-Newtonian Gravity. Available:https:Lunar Laser Ranging-a comprehensive probe of post-Newtonian gravity
40. Yuanbo Du, Rong Wei, Richang Dong. Progress of the portable rubidium atomic fountain clock in SIOM ... China Satellite Navigation Conference (CSNC); Proceedings. 2013;419-424. Available:https:Progress of the Portable Rubidium Atomic Fountain Clock in SIOM ...
41. Hänsch TW. Nobel Lecture: Passion for precision. Reviews of Modern Physics. 2006;78(4):1297–1309 DOI: 10.1103/revmodphys.78.1297
42. Einstein A. On the influence of gravitation on the propagation of light. Ann. D. Phys. 1911;35:898-908. Available:http:On the Influence of Gravitation on the Propagation of Light By A ...
43. Sagnac G. Sur la preuve de la réalité de l'éther lumineux par l'expérience de l'interférographe tournant. In: Comptes Rendus. 1913;157:S.1410–1413. Available:fr:Sur la preuve de la réalité de l'éther lumineux par l'expérience de l'interférographe tournant
44. Van Raamsdonk M. Building up spacetime with quantum entanglement. In: General Relativity and Gravitation. 2010;42(19): S.2323–2329. DOI: 10.1007/s10714-010-1034-0
45. Rovelli C, Smolin L. Discreteness of area and volume in quantum gravity, Nuclear Physics B, Band. 1995;442:S.593; Erratum. B. 1995;456:753. Available:https:Discreteness of area and volume in quantum gravity

Peer-review history:
The peer review history for this paper can be accessed here:
http://www.sdiarticle3.com/review-history/50248